Simulation Experiments for Determining Wind Data Requirements in the Tropics

C. T. GORDON, L. UMSCHEID, JR., AND K. MIYAKODA

Geophysical Fluid Dynamics Laboratory, NOAA, Princeton University, Princeton, N. J. 08540

(Manuscript received 2 February 1972, in revised form 28 April 1972)

ABSTRACT

Numerical simulation experiments are performed with a 9-level global general circulation model to help determine how much wind data in the tropics are needed for the reconstruction of meteorological fields. Prediction runs are updated every 12 hr with hypothetical data generated from the same model.

It is found that the asymptotic root mean square (rms) wind errors in the tropics, particularly in the 11S–11N "equatorial" latitude belt, fail to meet the GARP data requirements for the FGGE if surface pressure and temperature data alone are used for updating. The addition of tropical wind data at just two vertical levels leads to a significant, but insufficient, reduction of rms wind errors within the "tropics" (26S–26N); the largest errors remain near the equator. However, these errors become acceptably small if wind data are inserted at all 9 levels within the equatorial region. Another result is that insertion of tropical wind data at just two levels has a sizable influence upon wind errors even in the extratropics.

A critique of some implicit assumptions made in simulation experiments of the type we have performed is included.

1. Introduction

In response to a request by the Joint Organizing Committee (JOC) for the Global Atmospheric Research Program (GARP) contained in the Report of its Fifth Session at Bombay (1971), we have performed a series of numerical experiments for the Research Coordination and Planning Group (RCPG) on observing systems simulation. The principal objective is to help determine whether wind measurements will be necessary in the tropics. The observation system for the First GARP Global Experiment (FGGE) would be less costly if winds in the tropics could be derived from mass field information alone.

The concept of updating a numerical forecast with hypothetical data has already been demonstrated with some success. Examples include the work of Charney *et al.* (1969), Jastrow and Halem (1970), Williamson and Kasahara (1971), Talagrand and Miyakoda (1971), Bengtsson and Gustavsson (1971), and Messinger (1971). The principal differences among these various investigations has involved (i) model characteristics, (ii) variables to be updated and their domain, and (iii) method of data assimilation.

Our present purpose, however, is not to study methods of assimilation themselves, but rather to see how the errors of the assimilated fields depend upon the data set that is inserted. Although the question of dependence of the final asymptotic error level upon the insertion scheme is not precisely known, it has been studied to some extent. The comparison of an optimum interpolation method to a direct insertion method by Bengtsson and Gustavsson (1971) suggests little dependence. Meanwhile, in Messinger's (1971) study, optimization of smoothing properties of the time differencing scheme apparently yields about a 25% reduction in asymptotic global rms error. In any case, it is assumed that our asymptotic error levels would not be greatly reduced by using more sophisticated methods of insertion than used here upon the *same* data. As a working hypothesis, we also assume that numerical simulation experiments can provide the JOC with qualitative answers to their questions [see also Jastrow and Halem (1970)]. This assumption is reexamined in Section 7 with regard to the use of the hypothetical data, imperfections in our model, and model dependence of the results.

Basically, we find that the wind errors remain large in the tropics if tropical wind data are not used for updating. Moreover, extensive wind information is especially critical in the narrow "equatorial" belt (11S–11N). As expected, the winds adjust more readily at middle and high latitudes than in the "tropics" belt (26S–26N) to the mass field. But tropical wind data can influence the rms wind error in the extratropics (poleward of 26°), particularly in the winter hemisphere.

2. Characteristics of the general circulation model

A global general circulation model with an $N=24$ or an $N=48$ Kurihara mesh was available at GFDL. (N denotes the number of grid points from pole to equator.) Computational considerations dictated using

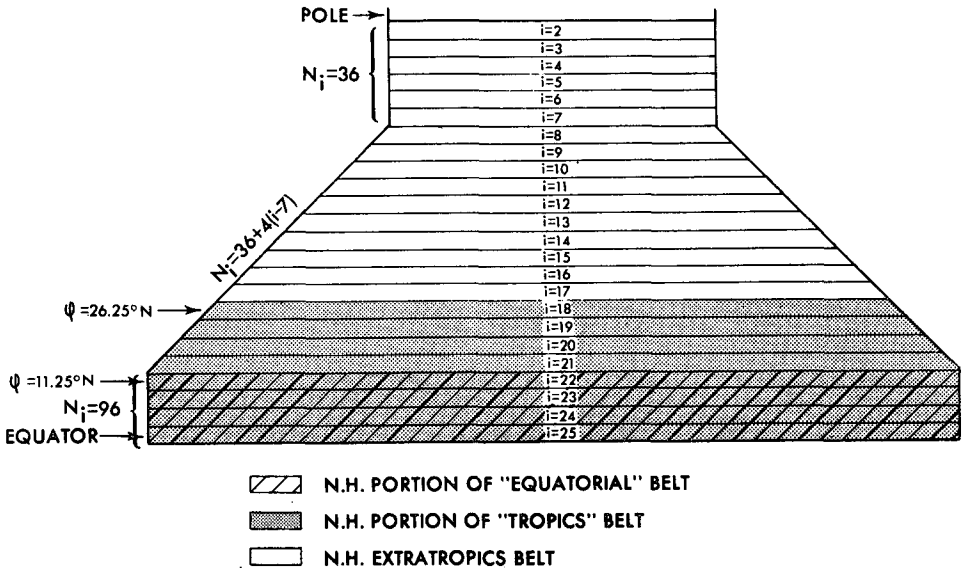

FIG. 1. The modified Kurihara grid. The number of grid points N_i for each row of the Northern Hemisphere is shown schematically. Also, the "equatorial," "tropics" and N.H. extratropics belts are delineated.

the coarser $N=24$ mesh which has a 417 km or 3.75° grid spacing in the meridional direction. Unfortunately, truncation errors were large near the poles where there are few grid points. Considerable improvement was achieved, however, by increasing the number of grid points in the longitudinal direction in polar regions and introducing the longitudinal smoothing technique of Umscheid and Sankar-Rao (1971). A schematic diagram of the modified grid used here is illustrated in Fig. 1. Note that this grid is rectangular in the polar smoothing region (36 grid points per row) and in the equatorial belt (96 grid points per row), and resembles a conventional Kurihara grid at intermediate latitudes. The vertical coordinate is $\sigma=p/p_s$, where p and p_s denote the pressure and surface pressure, respectively. The model has nine unequally spaced levels as depicted schematically in Fig. 2.

A very weak time filter (see Robert, 1965; Asselin, 1971) has been applied at each time step in conjunction with leap-frog time differencing. Its primary function is to couple the solutions at even and odd time steps.

The physics of the model is similar to that of the global general circulation models with the conventional Kurihara $N=24$ and $N=48$ grids discussed by Holloway and Manabe (1971) and by Miyakoda *et al.* (1971), respectively. Topography, land and sea contrast, moisture, convective adjustment, precipitation, a hydrologic cycle, a radiation calculation every 12 hr, and vertical diffusion of moisture and momentum in the boundary layer are all included. Another important feature is that the season is fixed and diurnal variation of insolation is neglected. For our particular experiments, the solar insolation is for the month of January, i.e., the Northern Hemisphere is the winter hemisphere.

One limitation of the model is that the $N=24$ grid is too coarse to fully resolve the flow particularly in the intertropical convergence zone (ITCZ). Secondly, given the irregular "modified Kurihara" grid, the numerical accuracy is probably somewhat less than second order, at least at some locations. The running time on the UNIVAC 1108 computer was 6.75 hr per model day.

3. The approach

Despite differences in the details, the procedure adopted here is similar to that of Charney *et al.* (1969). First, a hypothetical "control" forecast was made using leap-frog time differencing. The horizontal wind components u and v, the temperature T, and the

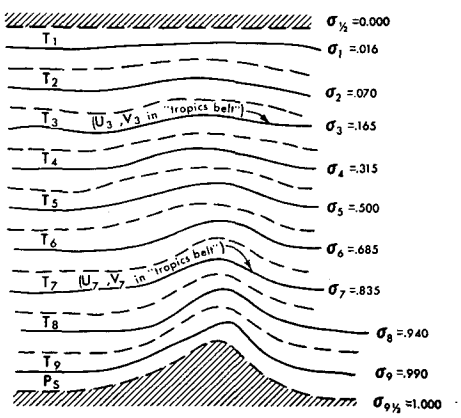

FIG. 2. Schematic diagram of the model's vertical representation, with values of $\sigma=p/p_s$ given at each of the nine interior levels and at the top and bottom boundaries. Updated variables are indicated for Exp. 2-ER.

mixing ratio r at nine σ levels, plus the surface pressure p_s, were extracted over the global domain at 2-hr intervals. These prognostic variables were stored on "control data" tapes. In turn, from the control data, "insertion" tapes containing the appropriate insertion data were generated for each updating experiment. The variables and their latitude domains to be inserted can be identified from the tape format. Also random and/or systematic errors have been incorporated into the insertion data for three of the experiments.

a. *Classification of experiments*

Five basic experiments with 12-hr updating were carried out and are summarized in Table 1. They are distinguished by type of hypothetical data to be inserted and its domain, e.g., type 1, 2 or 3, and by whether these data are perfect or are contaminated by hypothetical random and/or systematic errors. The suffix-ER indicates that the hypothetical data have been contaminated by error. The JOC has called only for experiments with contaminated data. But we thought that experiments with perfect data were extremely useful in clarifying the results. They also provided some comparison with previous investigations in which only temperatures and surface pressures were updated.

According to Table 1, no wind data were inserted in Exp. 1 or in Exp. 1-ER. However, as in all five experiments, both the surface pressure and temperatures at all levels were inserted at all grid points. In Exps. 2-ER, 3-ER and 3, horizontal winds at level 3 ($\sim$165 mb) and at level 7 ($\sim$835 mb) were also inserted at all grid points in the 26S–26N "tropics" belt. Meanwhile, in Exps. 3-ER and 3, additional wind data, i.e., horizontal winds at all levels, were inserted within the narrow 11S–11N "equatorial" belt. The updated variables for Exp. 2-ER have been depicted schematically in Fig. 2.

b. *Error specifications for inserted data*

Random and systematic temperature errors proposed by the JOC were incorporated into the insertion data for Exps. 1-ER, 2-ER and 3-ER. The systematic error, $\sin(2\varphi)\sin(4\lambda)$, where φ is the latitude and λ is the longitude, has an amplitude of 1C and is small near the equator. A separate, independently distributed sequence of random errors was generated for each of the variables u, v, T at each level. Each sequence of random errors belonged to a normalized rectangular (square wave shaped) probability density distribution with zero mean and appropriate cutoff limits. As expected, the rms of each rectangular distribution with zero mean was about $3^{-\frac{1}{2}}$ as large as the cutoff value.

The rms wind component errors proposed by the JOC were designated instead as cutoff limits. Thus, the cutoff (absolute maximum) error of a horizontal vector wind observation at level 3 or 7 in the tropics belt is 2.0 m sec^{-1} for Exp. 2-ER. Similarly, the cutoff error for the wind components u and v at levels 3 and 7 is 1.41 m sec^{-1}. The corresponding rms errors are, respectively, 1.15 and 0.82 m sec^{-1}. In Exp. 3-ER, these error limits still apply in the tropics belt at levels 3 and 7, except within the equatorial belt. There, winds were inserted at all levels with cutoff and rms errors one-half as large as the above values.

c. *Time differencing scheme for assimilation*

Leap-frog time differencing, plus a very weak time filter (see Robert, 1965; Asselin, 1971) were applied exclusively during the first 12 days of each experiment with the following exception. One forward difference step was carried out immediately after each data insertion. This speeded up the rate of error decrease considerably by eliminating a potentially large initial decoupling between the forecast and the inserted data.

TABLE 1. Classification of experiments.

Experiment	Data set	Error input	Update interval
Exp. 1	p_s at all grid points T at all levels, all grid points	None	12 hr
Exp. 1-ER	p_s at all grid points	None for p_s	12 hr
	T at all levels, all grid points	Systematic error$=1.0\sin 2\varphi \sin 4\lambda$ [°C] plus random error with 0.866C cutoff	
Exp. 2-ER	p_s at all grid points	None for p_s	12 hr
	T at all levels, all grid points	Systematic error$=1.0\sin 2\varphi \sin 4\lambda$ [°C] plus random error with 0.866C cutoff	
	u_3, v_3, u_7, v_7, at all grid points in tropics band $\lvert\varphi\rvert \leqslant 26.25°$	Random error with 1.41 m sec^{-1} cutoff for each wind component (2 m sec^{-1} for vector velocity magnitude)	
Exp. 3	Same as in Exp. 2-ER except for u, v at all levels and grid points in equatorial band $\lvert\varphi\rvert \leqslant 11.25°$	None	12 hr
Exp. 3-ER	Same as in Exp. 2-ER except for u, v at all levels and grid points in equatorial band $\lvert\varphi\rvert \leqslant 11.25°$	Same as in Exp. 2-ER except that in the equatorial band the random error has a 0.707 m sec^{-1} cutoff for each wind component (1.00 m sec^{-1} for vector velocity magnitude)	12 hr

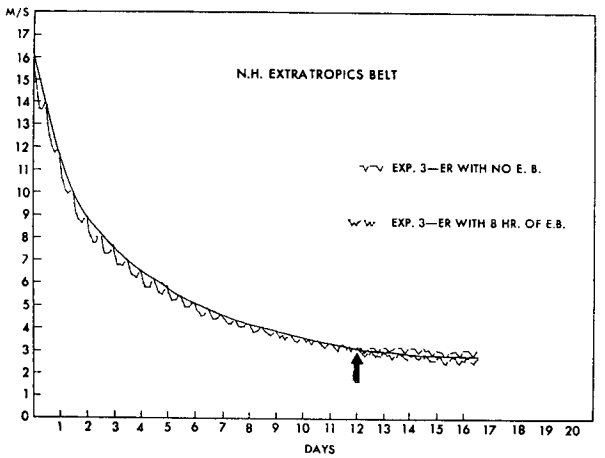

FIG. 3. Smoothing procedure and the effect of Euler backward (E.B.) differencing. Faint dots are rms wind errors at 2-hr intervals. A raw (smoothed) curve is obtained by connecting the dots (connecting the relative maxima of the dots). To the right of the arrow, the lower raw curve and the smoothed curve represent 8 hr of Euler backward time differencing after each insertion.

Beginning on model day 12, however, Euler backward (Matsuno) time differencing was performed for 8 hr after each data insertion in the hopes of reducing the error even more quickly and to see if the asymptotic rms vector wind error level itself would decrease. The unsmoothed Exp. 3-ER Northern Hemisphere extratropics curves for the forward difference and Euler backward methods may be compared in Fig. 3. The amount of improvement with the Euler backward method in the extratropics is typical for all runs. However, the improvement of the rms wind error in the tropics belt was very slight.

d. Initial state

The initial state for all experiments was arbitrarily specified as the control run solution at day 10.58. Persistence curves for control run temperatures and winds indicated that the solutions at days 0 and 10.58 differed as much as two randomly chosen states. Thus, the initial experimental errors were equal to these large values. Insertion of data was made at intervals of 12 model hours, and each updating experiment was run 16–20 days.

4. Methods of verification

Every two model hours, the prognostic variables at all levels and grid points were written on "experimental data" tapes for each experimental run. These tapes were later verified against the corresponding "control data" tapes. The time evolution and asymptotic values of the rms temperature and vector wind errors have been analyzed in the form of 1) (mass weighted) vertical averages and vertical profiles for various latitude domains, and 2) latitudinal profiles of vertical averages. Also, visual comparisons were made between control and experimental synoptic maps of the 500-mb geopotential height field, and the 165-mb streamline pattern.

a. Latitude domains

Whereas the global domain is traditionally analyzed, separate verifications for (i) the Northern Hemisphere (N.H.) [or Southern Hemisphere (S.H.)] extratropics (30°–90°), (ii) the "tropics" belt, and (iii) the "equatorial" belt are probably more informative. These belts are delineated in Fig. 1. Recall that wind data are inserted in the tropics and equatorial belts for Exps. 2-ER, 3-ER and 3, but never in the N.H. (or S.H.) extratropics.

b. Construction of smoothed curves of rms error vs time

Rms errors have been plotted for various latitude domains at intervals of two model hours, i.e., at 0, 2, 4, 6, 8 and 10 hr after each insertion. Smoothed curves have then been obtained by connecting adjacent relative maxima. The process is illustrated for curves of vertically averaged rms vector wind error vs time in Fig. 3 and the lower half of Fig. 4 for the N.H. extratropics and the equatorial belts, respectively.

The raw error curves for a given latitude belt exhibit only weak discontinuities at insertion time if wind data are not directly inserted there. This applies to all curves in the N.H. extratropics, and to the Exp. 1-ER (and Exp. 1) curves in the equatorial or tropics belts. Moreover, in Fig. 3 (and in Fig. 4), the rms wind error decreases for about 4-6 hr after each data insertion and then increases. This suggests that 6-hr updating would be more efficient than 12-hr updating. In contrast, the Exp. 2-ER and Exp. 3-ER (and Exp. 3) curves exhibit sharp discontinuities in the equatorial and tropics belts at data insertion times, and error growth between insertions.

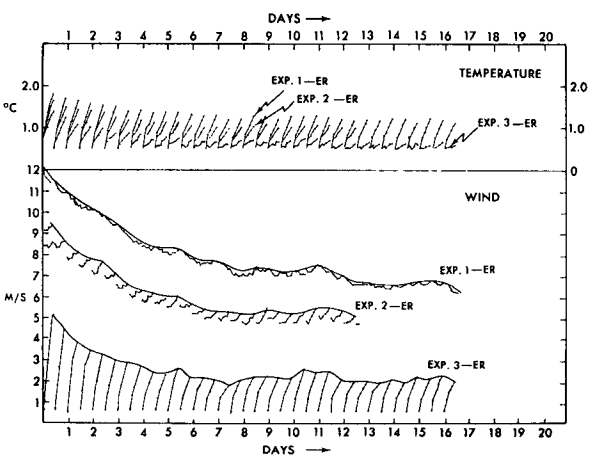

FIG. 4. Rms vector wind and temperature errors for the equatorial belt. Results are shown only for the experiments with imperfect data. Raw temperature error curves (above) and both raw and smoothed wind error curves (below) are plotted.

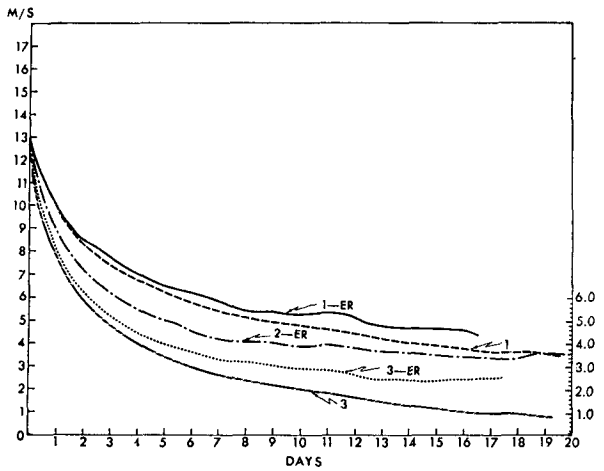

FIG. 5. Global vertically averaged rms vector wind error vs time for five experiments.

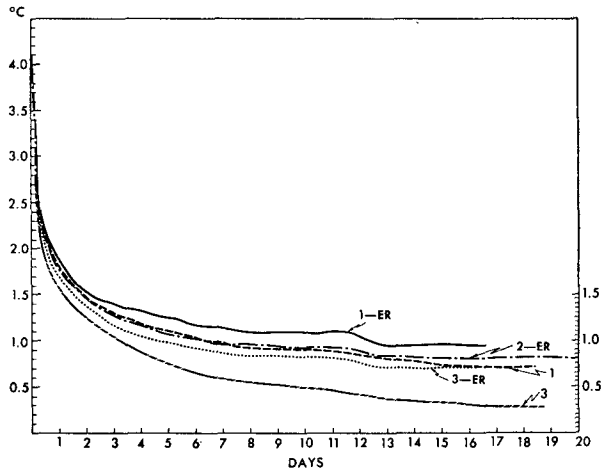

FIG. 6. Global vertically averaged rms temperature error vs time for five experiments.

5. Results

Smoothed curves of vertically averaged global rms wind errors and temperature errors vs time are plotted in Figs. 5 and 6. The final error levels should be regarded as quasi-asymptotic. Note that the vertically averaged rms vector wind error E_w is plotted, where $E_w=(E_u^2+E_v^2)^{\frac{1}{2}}$, and E_u and E_v are the vertically averaged rms errors of the u and v wind components. Roughly speaking $E_u \approx 0.7\ E_w$, i.e., globally, the error variance is distributed almost equally between the u and v components. The quasi-asymptotic global, vertically averaged rms vector wind errors for Exps. 1-ER, 2-ER and 3-ER are 4.4, 3.4 and 2.4 m sec^{-1}, respectively. The corresponding global rms temperature errors are 0.92, 0.79 and 0.72K.

The experiments Exp. 1 and Exp. 1-ER correspond most closely to the type previously performed by various investigators. Of these, Exp. 1 is a better analog, since Exp. 1-ER contains *systematic* as well as random errors. The curves of Kasahara and Williamson (1972) for an Exp. 1 type experiment indicate that the global vertically averaged rms error E_u of the zonal wind component is approximately 0.8 m sec^{-1} in the asymptotic limit. The corresponding asymptotic value for our Exp. 1 is $E_u \approx 0.7\ E_w \approx 2.5$ m sec^{-1}. Thus, when perfect temperature and surface pressure (mass field) information are inserted alone, our asymptotic rms wind error is considerably higher than Williamson and Kasahara's.

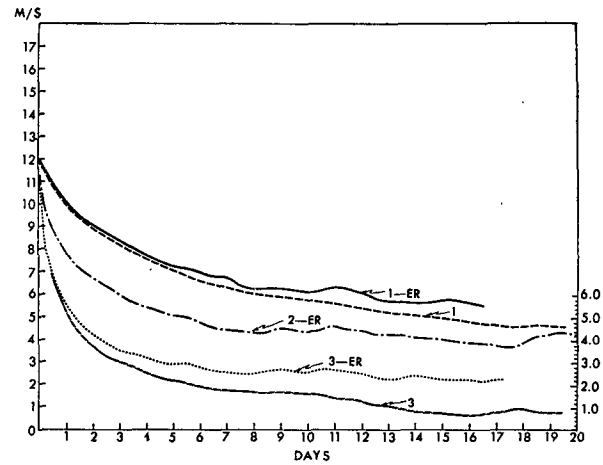

FIG. 7. Vertically averaged rms vector wind error in the tropics belt vs time for five experiments.

While the reason is not clear, it is more likely related to differences in model characteristics than in the method of insertion.

a. Rms wind and temperature error analysis by latitude domain

The quasi-asymptotic, vertically averaged rms vector wind errors for various latitude domains are summarized in Table 2 for all five experiments. After nearly 20 days

TABLE 2. Asymptotic vertically averaged rms vector wind errors (m sec^{-1}) for days 16.5 and 19.5 (in parentheses).

	Exp. 1-ER	Exp. 2-ER		Exp. 3-ER	Exp. 1		Exp. 3	
Equatorial belt	6.3	4.6	(5.4)	1.8	5.7	(5.9)	0.5	(0.7)
Tropics belt	5.4	3.8	(4.3)	2.1	4.7	(4.6)	0.7	(0.8)
N.H. extratropics belt	3.6	3.1	(2.9)	2.7	2.8	(2.5)	1.3	(0.9)
S.H. extratropics belt	3.2	2.8	(2.5)	2.8	1.7	(1.4)	0.9	(0.7)
Global	4.4	3.4	(3.6)	2.4	3.6	(3.5)	0.9	(0.8)

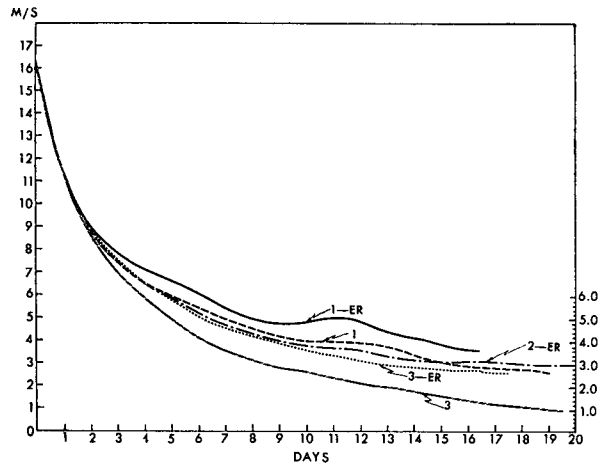

FIG. 8. Vertically averaged rms vector wind error in the N. H. extratropics belt vs time for five experiments.

of insertion, the rms wind errors have leveled off in the tropics and equatorial belts, but not quite in the N.H. (and S.H.) extratropics.

In the tropics (see Table 2), the quasi-asymptotic rms wind errors (m sec^{-1}) are 5.4 for Exp. 1-ER, $\gtrsim$3.8 for Exp. 2-ER, 2.1 for Exp. 3-ER, 4.6 for Exp. 1, and 0.7 for Exp. 3. The approach to these quasi-asymptotic values is illustrated in Fig. 7. Clearly, in Exps. 1-ER and 1, which utilize imperfect and perfect mass field information, respectively, the rms wind errors are too large to meet the GARP data requirements for the FGGE.[1] Even in Exp. 2-ER, which has tropical wind insertion at only two levels all the way to the equator, the error levels off too high, especially near the equator. Conversely, with additional wind data at all levels near the equator, the growth of wind error throughout the tropics belt remains within tolerable limits between insertions. According to Table 2, the quasiasymptotic rms wind errors for Exps. 1-ER and 2-ER are about 1 m sec^{-1} higher in the equatorial belt than in the tropics belt.

The unsmoothed curves in the top half of Fig. 4 give some insight as to how the rms temperature errors in the equatorial belt approach quasi-asymptotic values. With increasing time, the rate of error growth after each insertion becomes much flatter in Exp. 3-ER than in either Exps. 1-ER or 2-ER.

Consulting Table 2 again, the quasi-asymptotic values of rms wind error in the N.H. extratropics are 3.6 for Exp. 1-ER, 2.9 for Exp. 2-ER, $\lesssim$2.7 for Exp. 3-ER, 2.5 for Exp. 1, and 0.9 ($E_u \approx 0.6$ m sec^{-1}) for Exp. 3. The error in Exp. 1 and in Exp. 3 is still slowly decreasing. The asymptotic errors tend to be somewhat lower in the less active Southern (summer) Hemisphere. Comparing Figs. 7 and 8, the rms wind error curves flatten out sooner in the tropics than in the N.H. extratropics.

A particularly interesting result (see Fig. 8) is that the vertically averaged rms wind error is substantially reduced in the N.H. extratropics after several days if wind data are inserted at just two levels in the tropics belt (compare Exps. 1-ER and 2-ER). Insertion of 9 levels of wind data in the equatorial belt (Exp. 3-ER) leads to a further error reduction of somewhat smaller magnitude in the N.H. extratropics after about 10 days. Incidentally, the bulge in the Exp. 1-ER curve (and the Exp. 1 curve) at day 11 reflects a sluggish adjustment to a rather rapid change in the 500-mb geopotential height pattern of the control run. At about this time one intense closed low was dying out while another was developing downstream.

The relative importance of error-free temperature data (Exp. 1) vs contaminated temperature and tropical wind data (Exps. 2-ER and 3-ER) is best estimated from the asymptotic error states (see Table 2). In the N.H. extratropics, the quasi-asymptotic rms wind errors are comparable for Exps. 1 and 3-ER but larger for Exp. 2-ER. For wind determinations in the S.H. extratropics, error-free temperature data are much superior to contaminated temperature and tropical wind data. Meanwhile, the quasi-asymptotic rms temperature error (not shown) is lower for Exp. 1 in both extratropics regions. Quantitatively, the above results could easily depend upon the error bounds on the inserted wind data in Exps. 2-ER and 3-ER. But further analysis is beyond the scope of the present investigation.

b. Latitudinal distribution of the asymptotic wind errors

The quasi-asymptotic, vertically averaged rms vector wind error is plotted as a function of latitude in Fig. 9 for five experiments. The most striking feature about Fig. 9 is the behavior of the various experiments in

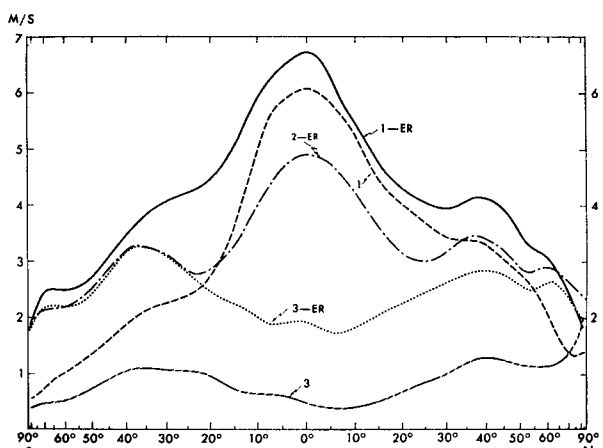

FIG. 9. Vertically averaged quasi-asymptotic rms vector wind error vs latitude at day 16, hour 10, for five experiments.

[1] The minimum acceptable standard proposed by the JOC is a 2 m sec^{-1} *cutoff* error for each wind component in the tropics (3 m sec^{-1} in middle and high latitudes).

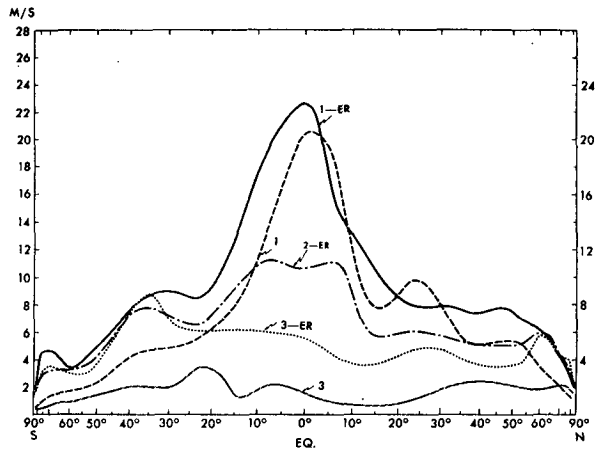

FIG. 10. Maximum error of the u_3 wind component vs latitude at day 16, hour 10, for five experiments. Three-point smoothing has been applied.

the tropics. The curvature of the error curves for Exp. 1-ER, Exp. 1, and even Exp. 2-ER is concave upward near the equator. Moreover, the rms error near the equator exceeds 6 m sec^{-1} in both Exps. 1-ER and 1, and 5 m sec^{-1} in Exp. 2-ER. Clearly, the vertically averaged rms vector wind error remains unacceptably large *near the equator* if winds are inserted at only *two levels* in the equatorial belt. In contrast, the rms vector wind error is only about 2 m sec^{-1} at the equator for Exp. 3-ER in which winds are updated at all levels in the equatorial belt.

Fig. 10 illustrates the absolute maximum error (somewhat smoothed) of the u_3 wind component vs latitude for the same day as in Fig. 9. Both sets of curves exhibit qualitatively similar behavior. However, the disparity between absolute maximum errors is even greater than that between rms errors for the five experiments. The unsmoothed absolute maximum error for Exp. 1-ER was actually 28 m sec^{-1}, just south of the equator, i.e., about four times larger than the rms error there. That value is larger than the cutoff value of a rectangular distribution having the equatorial rms value of Fig. 9. In other words, the output errors are distributed differently than the input errors.

Furthermore, in Exp. 1 and particularly in Exp. 1-ER, huge error maxima occasionally flare up near the equator. For example, on day 14, the absolute maximum grid point error of u_3 exceeded 50 m sec^{-1} in Exp. 1-ER.

The N.H. extratropics crossover point between the Exp. 1 and Exp. 3-ER rms wind error curves in Fig. 9 has the following interpretation. Temperature and tropical wind data with the errors specified by Exp. 3-ER have more impact in the N.H. extratropics than does *perfect* temperature data alone equatorward of the crossover point. This crossover point for wind error is somewhat poleward of the corresponding N.H. crossover point for temperature error (Fig. 12).

Note that the Southern is closer than the Northern Hemispheric crossover point to the equator in Figs. 9 and 10. Also, the ratio of rms or maximum wind error for the Northern vs the Southern Hemisphere at a given latitude in the extratropics is larger if wind information is not inserted (see Exp. 1-ER) in the tropics. We speculate that these two features of Figs. 9 and 10 reflect the deeper penetration of tropical influences (e.g., the Hadley circulation) into the Northern, i.e. winter, Hemisphere. The quality of wind information propagated from the tropics may determine whether the effect upon the extratropics is beneficial or detrimental.

The skewness of error about the equator for the Exp. 3-ER curves of Figs. 9 and 10 may be associated with the greater convective activity (precipitation) at southern equatorial latitudes. The latitudinally skewed precipitation distribution (not shown) is reasonable for the month of January. Its effect is evidently masked in the other curves by the effect of zero Coriolis parameter at the equator, i.e., a lack of adjustment of the wind to the mass field, suggested from linearized adjustment theory.

c. *Vertical distribution of the asymptotic wind errors*

In Fig. 11, vertical profiles of quasi-asymptotic rms vector wind error are drawn for both the N.H. extratropics and tropics belts at day 16, hour 10. In the N.H. extratropics, nearly all rms error curves attain a maximum at the highest stratospheric level where the model's polar night jet is too intense. The minimum rms error for all curves is found at the level nearest the surface. As in the vertically averaged case, the rms wind error at many levels of the N.H. extratropics is significantly reduced if wind data are inserted at two levels in the tropics belt, and at two or especially nine levels in the equatorial belt. At most levels, the error reduction exceeds 1.25 m sec^{-1} in the error-free cases

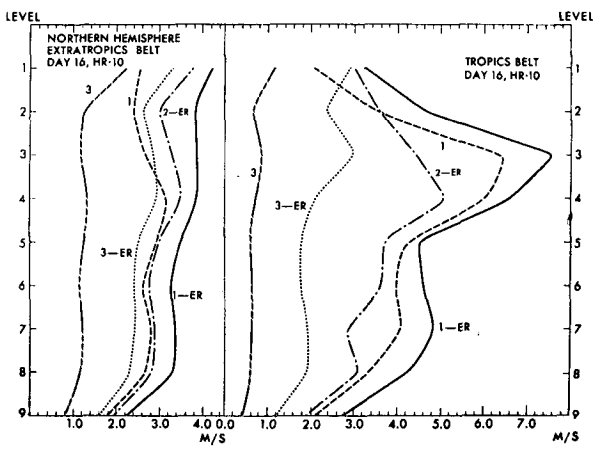

FIG. 11. Vertical profiles of rms vector wind error at day 16, hour 10, in both the N.H. extratropics and in the tropics belts for five experiments.

and approaches 1 m sec^{-1} in the error-contaminated cases. The errors of Exps. 3-ER and 1 are of roughly the same magnitude. There is a crossover point between levels 3 and 4. The Exp. 2-ER curve lies between the Exp. 1-ER and Exp. 3-ER curves.

In the tropics, both Exps. 1 and 1-ER have pronounced peaks of rms wind error at level 3 and smaller peaks at level 7 (see Fig. 11). However, the eddy kinetic energy in the tropics is a maximum at level 3 in the Manabe *et al.* (1970) model. Thus, we would expect a normalized error curve to be flatter. The peak at level 3 persists in Exp. 3-ER, but is much weaker. The Exp. 2-ER peak is at level 4, since wind data are inserted at level 3 but not at level 4. Below level 2, the rms wind error is significantly smaller in Exp. 3-ER than in Exps. 1-ER or 2-ER. The wind error in Exp. 3 is small and rather uniform with height.

d. Latitude distribution of the asymptotic temperature errors

The quasi-asymptotic rms temperature error vs latitude is illustrated in Fig. 12 for five experiments at day 16, hour 10. The patterns are similar to those of the rms wind errors in Fig. 9. One quantitative difference is that the relative gap at the equator between Exps. 1 and 3-ER is less for temperature than for wind. Nevertheless, the huge wind errors near the equator evidently have a detrimental feedback effect upon the temperature there.

e. Vertical distribution of the asymptotic temperature errors

Vertical profiles of quasi-asymptotic rms temperature error, analogous to those of Fig. 11 for wind, appear in Fig. 13. Note that the positions of the Exp. 1 and Exp. 3-ER curves are reversed in the tropics as compared to the N.H. extratropics, the error for Exp. 1 being larger in the tropics. For these experiments, the

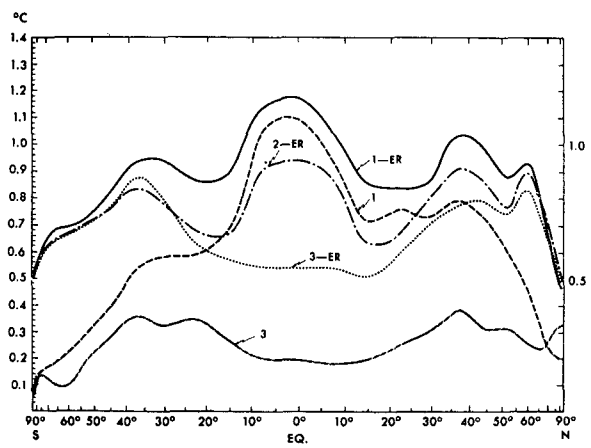

FIG. 12. Vertically averaged quasi-asymptotic rms temperature error vs latitude at day 16, hour 10, for five experiments.

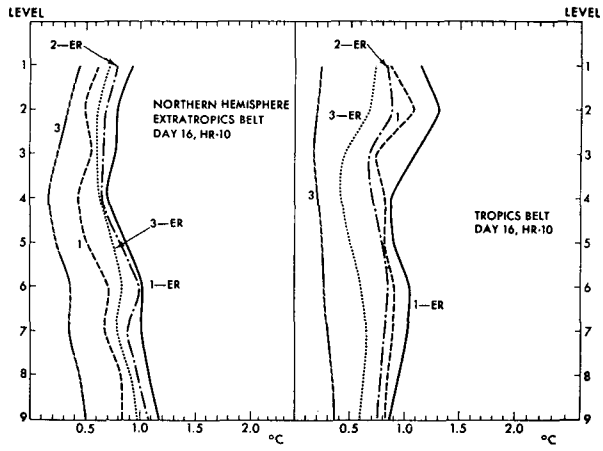

FIG. 13. Vertical profiles of rms temperature error at day 16, hour 10, in both the N.H. extratropics and in the tropics for five experiments.

maximum rms temperature errors at level 2 in the tropics are rather pronounced. As the surface is approached, the temperature error increases in the N.H. extratropics but decreases in the tropics. We speculate that this could reflect, in part, the different proportioning of land to sea surface area in the two regions, since the sea surface temperature specification is fixed.

f. Comparison of 500-mb geopotential height analyses

Having described various error statistics, a visual comparison between the control and experimental runs is now presented. First, the 500-mb geopotential height field is shown in Fig. 14 for day 16, hour 10, in the form of a control map and two difference maps. The Exp. 3-ER minus control difference map is better than the Exp. 1-ER minus control map, even in the tropics. This reflects the positive feedback effect of wind data on the mass field. At the same time, the two difference maps are rather highly correlated. Outside the tropics, errors as large as 80 m are found on the Exp. 1-ER vs control *difference* map at 500 mb. However, these are predominantly phase errors (slight shifts in the positions of troughs and ridges) rather than amplitude errors and may be associated with the systematic temperature error input. Nevertheless, the agreement between the Exp. 1-ER map itself (not shown) and the control map is quite good. The agreement between the Exp. 1-ER and control maps is not as good at 1000 mb.

g. Comparison of streamline patterns at level 3

The streaks in Fig. 15 were produced utilizing a computer program developed by D. Johnson at GFDL. They trace out streamlines of the horizontal wind field at level 3 for the control run, Exp. 1-ER and Exp. 3-ER. Observe that the Exp. 3-ER and control patterns are in better agreement than the Exp. 1-ER

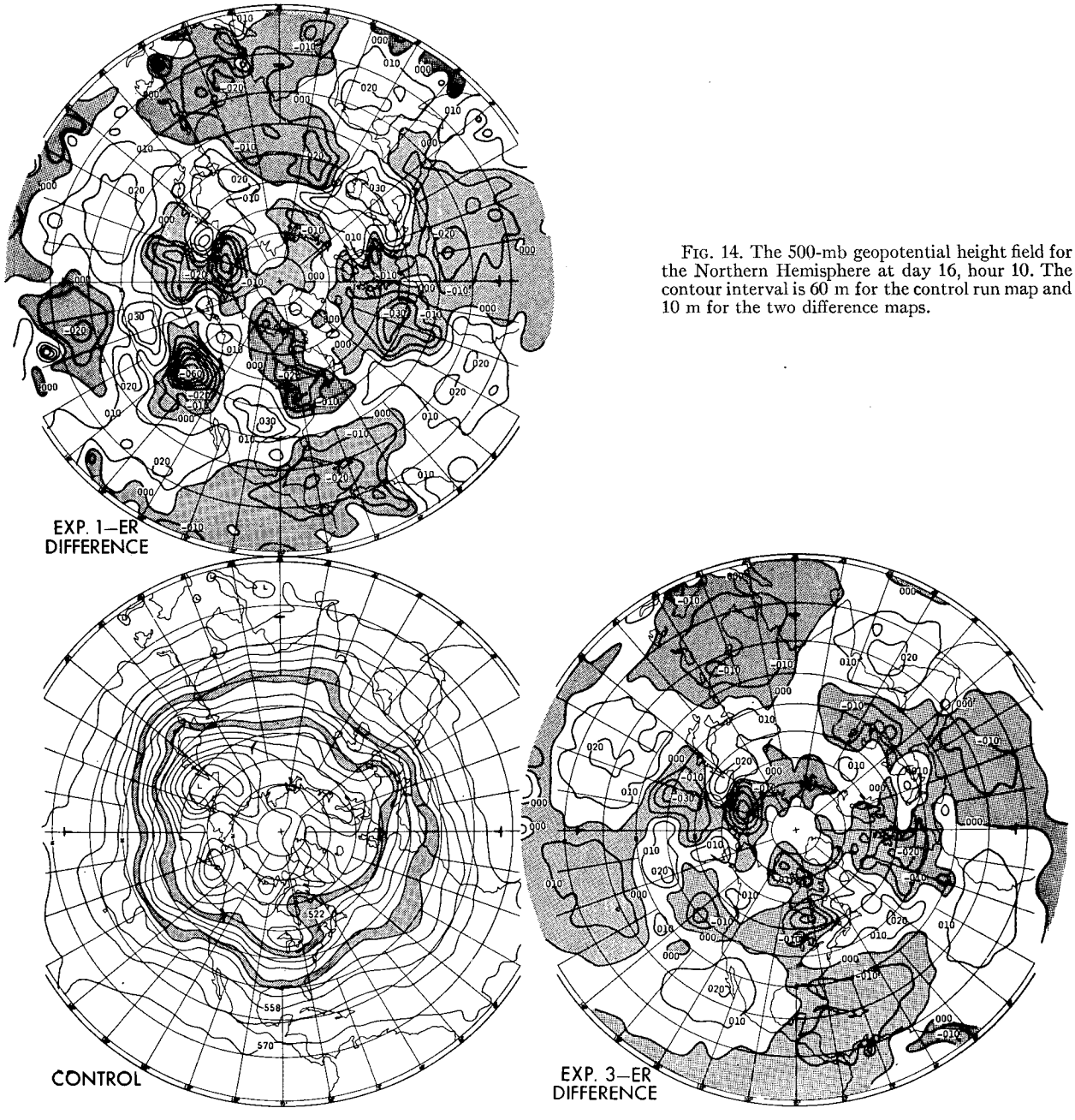

FIG. 14. The 500-mb geopotential height field for the Northern Hemisphere at day 16, hour 10. The contour interval is 60 m for the control run map and 10 m for the two difference maps.

and control patterns near the equator. Errors in the Exp. 1-ER streamlines are most noticeable at moderately small wavelengths.

h. Precipitation verification

We have also looked at mixing ratio and precipitation verifications for the extreme experiments Exp. 1-ER and Exp. 3. Mixing ratios are, of course, prognostic variables. The rms mixing ratio error decreases approximately monotonically with time. As anticipated, the reduction is more rapid in Exp. 3 than in Exp. 1-ER, especially in the tropics. However, by day 16, no significant net reduction in *rms precipitation* has occurred in either experiment. This situation prevails not only in the tropics but even in the extratropics. Since precipitation tends to be a small-scale phenomenon, perhaps the rms precipitation verification is a poor indicator of precipitation predictability. The role

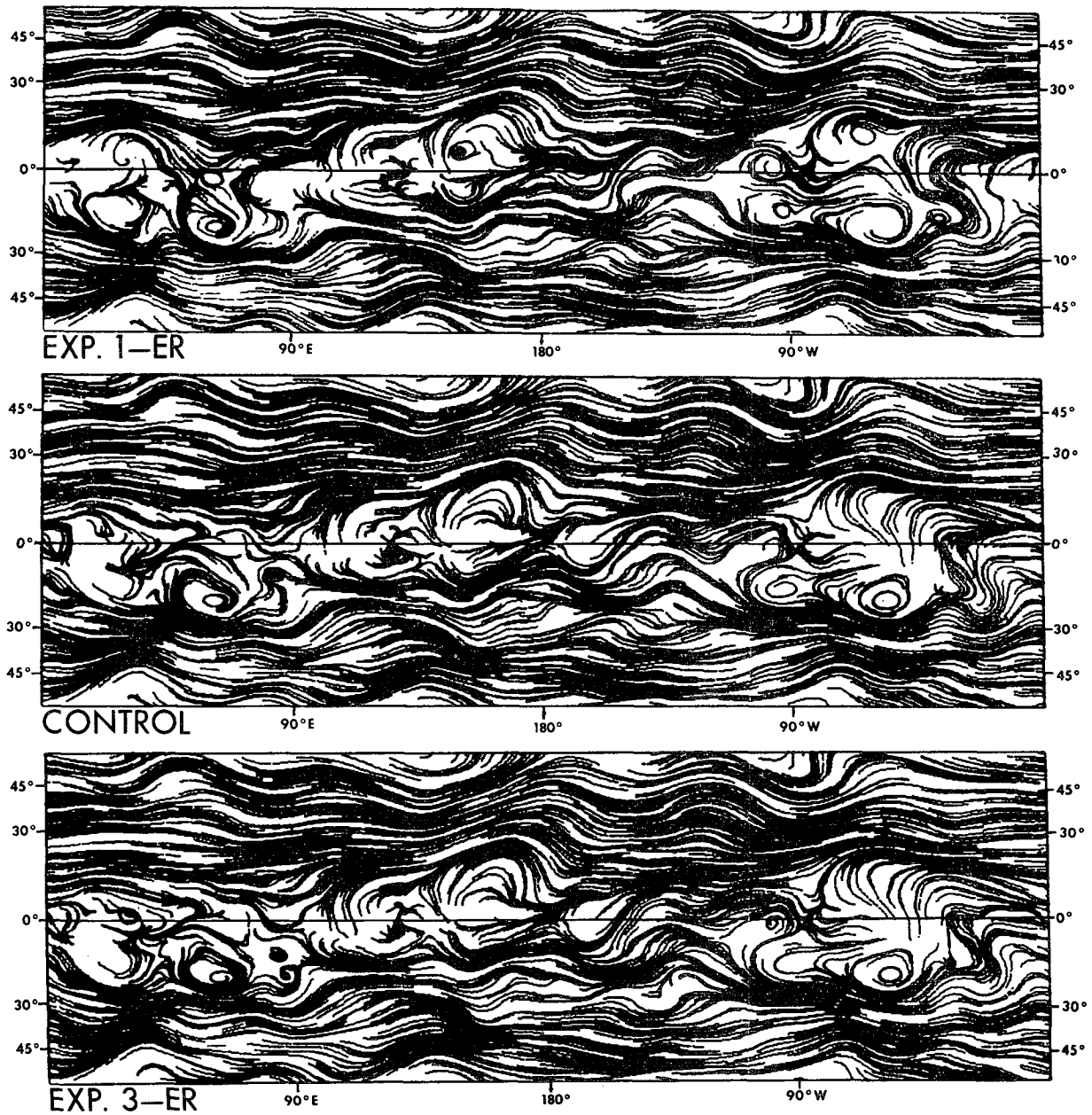

FIG. 15. Streamline patterns of the horizontal wind field V_3 at level 3 at day 16, hour 10 for the control run, Exp. 1-ER and 3-ER. The latitude domain is 56N (top) to 56S (bottom).

of precipitation in the adjustment process warrants further investigation.

6. Conclusions

Based upon our numerical simulation experiments, the data of Exp. 3-ER comes closer than that of Exps. 1-ER or 2-ER to the GARP data requirements for the tropics. The equatorial belt is especially troublesome. If no winds are specified in the tropics, the rms wind errors in the equatorial belt remain large, the asymptotic vertically averaged value for the tropics being 5.4 m sec^{-1}. The error is greatest at the 150–200 mb level. Insertion of winds at only two levels in the tropics helps somewhat, but not enough, particularly within 10–15° of the equator. By adding winds within the equatorial belt at all nine levels, the asymptotic rms wind error for the tropics is greatly reduced to 2.1 m sec^{-1} (Figs. 9 and 10). This result indicates that detailed wind information is absolutely necessary near the equator. The inference for the real atmosphere is that the mass field would probably tend to adjust to

the wind field near the equator. On the other hand, the winds should tend to adjust to the mass field at higher latitudes. This is not inconsistent with the predictions from linearized adjustment theory.

Another conclusion is that improved adjustment of winds also occurs in the extratropics, when tropical winds are inserted at just two levels. Additional equatorial wind information yields a somewhat smaller further reduction of wind error in the extratropics. Although the precise mechanism of coupling is not well understood, our results suggest that the tropics could influence the extratropics in the real atmosphere after several days. The coupling appears strongest in the winter hemisphere.

7. Critique

Some questions may be raised concerning various implicit assumptions made in the numerical simulation experiments:

Can meaningful results be obtained with hypothetical "identical twin" type data? Since the asymptotic error limits would probably be larger if real data were utilized, good results with hypothetical data may be a minimum requirement, at least for a given model.

Can the dependence of asymptotic error levels upon the data set and upon the method of assimilation be separated? In the present study, introduction of Euler backward differencing did reduce the asymptotic error somewhat in the extratropics, but only very slightly in the tropics, and did not affect our basic conclusions. It is not known whether a more sophisticated updating scheme would yield significantly lower asymptotic errors in the tropics when applied to the same data.

Are the conclusions of numerical simulation experiments model independent? It was originally thought that the difference between a control and experimental solution might not be terribly sensitive to the model even if the control solution itself were. However, results obtained from the GFDL model and the NCAR model (see Kasahara and Williamson, 1972) suggest that model dependency is somewhat stronger than originally anticipated. Thus, the model characteristics most responsible for the discrepancies should be identified. At present, however, our comments can only be speculative. Compared to the NCAR model, the GFDL model has more vertical resolution, somewhat higher horizontal resolution, and significantly more activity in the tropics, which could help to explain its higher asymptotic errors. The relative reduction of error in the tropics for temperature and surface pressure updating alone (Exp. 1-ER) is rather similar for both models. We realize that an error-growth experiment with our model would be useful, and hope to perform such an experiment at a future date.

Another question immediately arises, i.e., how realistic are the numerical models? The model used in these experiments is similar to the one discussed by Manabe *et al.* (1970). The climatology of their tropical tropospheric circulation is in fairly good agreement with the existing observations. This is encouraging to us. Nevertheless, the model has many defects. For instance, the horizontal and vertical grid resolution is poor, so the truncation error is probably still large. In particular, an excessive amount of gravity waves is possibly generated in the tropics. It would be instructive to compare the predictions of various models with observations in the tropics, when available.

Some refinements of the present study are desirable. First, a spectral analysis of the rms errors would confirm which spatial scales contain the largest errors. Presumably, the error variance is not concentrated near the grid length scale. Second, normalized errors could be computed from knowledge of the natural variability of our control solutions. Third, two other experiments similar to Exp. 3-ER could be attempted, one having reduced horizontal and vertical density of data, the other having reduced vertical density of data and increased frequency of data insertion.

Acknowledgments. The authors would like to thank the many people who contributed to this study. Drs. J. Smagorinsky and S. Manabe offered valuable comments and encouragement. Mr. L. Holloway provided background computer programs of the N24 global general circulation model. Mr. D. Johnson and Mr. J. Welsh developed the streamline analysis program, which was modified by Mr. D. Hembree. The experiments and rms verification analyses were run by Mr. I. Shulman and the 500-mb geopotential and the level 3 streamline analysis programs by Mr. J. Pollock. The diagrams were plotted by Mr. T. Mauk, drafted by Mr. P. Tunison and Mr. R. Richards, and photographed by Mr. J. Conner, Jr., Mrs. J. Ferko and Mrs. Y. Rowns typed the manuscript.

REFERENCES

Asselin, R., 1971: A time filter for time integrations. *Mon. Wea. Rev.* (in press).

Bengtsson, L., and N. Gustavsson, 1971: An experiment in the assimilation of data in dynamical analysis. *Tellus*, **23**, 328–336.

Charney, J., M. Halem and R. Jastrow, 1969: Use of incomplete historical data to infer the present state of the atmosphere. *J. Atmos. Sci.*, **26**, 1160–1163.

Holloway, J. L., Jr., and S. Manabe, 1971: Simulation of climate by a global general circulation model, I. Hydrologic cycle and heat balance. *Mon. Wea. Rev.*, **99**, 335–370.

Jastrow, R., and M. Halem, 1970: Simulation studies related to GARP. *Bull. Amer. Meteor. Soc.*, **51**, 490–513.

Joint Organizing Committee (JOC) of the Global Atmospheric Research Programme, 1971: Report of the Fifth Session of the JOC. World Meteorological Organization, Bombay, India, 15–16.

Kasahara, A., and D. Williamson, 1972: Evaluation of tropical wind and reference pressure measurements. Numerical experiments for observing systems. *Tellus*, **24**, 100–115.

Manabe, S., J. L. Holloway, Jr. and H. Stone, 1970: Tropical circulation in a time-integration of a global model of the atmosphere. *J. Atmos. Sci.*, **27**, 580–613.

Messinger, F., 1971: Computation of the wind by forced adjustment to the height field (1971). Dept. of Meteorology, UCLA, Grant NGR-05-007-091.

Miyakoda, K., R. W. Moyer, H. Stambler, R. H. Clarke and R. F. Strickler, 1971: A prediction experiment with a global model in the Kurihara grid. *J. Meteor. Soc. Japan*, **49**, 521–536.

Robert, A. J., 1965: The behavior of planetary waves in an atmospheric model based on spherical harmonics. Arctic Meteor. Res. Group, McGill University, Publ. Meteor. No. 77, 59–62.

Talagrand, O., and K. Miyakoda, 1971: The assimilation of past data in the meteorological dynamical analysis, Part II. *Tellus*, **23**, 318–327.

Umscheid, L., Jr., and M. Sankar-Rao, 1971: Further tests of a grid system for global numerical prediction. *Mon. Wea. Rev.* **99**, 686–690.

Williamson, D. L., and A. Kasahara, 1971: Adaptation of meteorological variables forced by updating. *J. Atmos. Sci.*, **28**, 1313–1324.